Investigations on sound energy decays and flows in a monumental mosque

Zühre Sü Gül[a)]
Department of Architecture, Middle East Technical University, Ankara, 06800, Turkey

Ning Xiang
Graduate Program in Architectural Acoustics, School of Architecture, Rensselaer Polytechnic Institute, Troy, New York 12180, USA

Mehmet Çalışkan
Department of Mechanical Engineering, Middle East Technical University, Ankara, 06800, Turkey

(Received 24 July 2015; revised 2 April 2016; accepted 20 May 2016; published online 15 July 2016)

This work investigates the sound energy decays and flows in the Süleymaniye Mosque in İstanbul. This is a single-space superstructure having multiple domes. The study searches for the non-exponential sound energy decay characteristics. The effect of different material surfaces and volumetric contributions are investigated using acoustic simulations and *in situ* acoustical measurements. Sound energy decay rates are estimated by Bayesian decay analysis. The measured data reveal double- or triple-slope energy decay profiles within the superstructure. To shed light on the mechanism of energy exchanges resulting in multi-slope decay, spatial sound energy distributions and energy flow vectors are studied by diffusion equation model (DEM) simulations. The resulting sound energy flow vector maps highlight the contribution of a sound-reflective central dome contrasted with an absorptive carpeted floor in providing delayed energy feedback. In contrast, no multi-slope energy decay pattern is observed in DEM simulations with a bare marble floor, which generates a much more diffuse sound field than in the real situation with a carpeted floor. The results demonstrate that energy fragmentation, in support of the non-exponential energy decay profile, is due to both the sound absorption characteristics of materials and to their distributions, as well as to relations between the subvolumes of the mosque's interior. © *2016 Acoustical Society of America*.
[http://dx.doi.org/10.1121/1.4953691]

[MV] Pages: 344–355

I. INTRODUCTION

The present work investigates acoustic coupling in a mosque having a multi-domed superstructure, which is capable of causing non-exponential decay of its sound field. Research on mosque acoustics and room acoustics involving coupling or coupled spaces are key topics involved in this study. The literature on mosque acoustics falls into three main categories. The first category comprises assessments of single mosques,[1,2] comparisons between different mosques,[3] and comparisons of mosques to churches.[4,5] The second category concerns the renovation of existing mosques[6–8] and the acoustic design of the new generation of mosques.[9] These studies discuss the acoustic design process and solutions to overcome acoustic defects. The third category includes investigations of real or virtual mosques[10] and review studies[11] that focus on acoustic design criteria for this specific type of building.

By promising a compromise between the competing acoustic conditions of reverberance and clarity, coupled spaces have aided acousticians in the design of concert halls and multi-purpose auditoriums.[12] The acoustic consequence of coupled spaces is a non-exponential decay of the sound energy. Theoretical studies of non-exponential sound energy decay include statistical theory,[13,14] statistical energy analysis,[15–17] diffusion equation modeling,[18–20] wave theory,[21,22] and geometrical acoustics.[23–25] Different models have differing advantages and limitations. Selecting the model for any situation is, therefore, a critical decision. Quantification of the degree of acoustical coupling is a further challenging task. Visual inspection, comparison of linear-fits of different portions of logarithmic decay functions, and application of ratio-based quantifiers without taking their absolute values into account are scientifically ineffective,[26,27] especially when the decay profile has more than two slopes. The present study uses Bayesian probabilistic inference, which is an efficient tool for estimating key characteristics of multiple slope sound energy decays.[27,28]

The acoustics of coupled rooms have previously been investigated in medium[29] and large scale[16,17] Christian worship spaces, but not in mosques with their distinctive design features. One of the major differences between cathedrals (or basilicas) and mosques is that the former have a basilican or rectangular plan layout and the volume is divided into many sub-spaces. The coupling of reverberant sub-spaces such as side aisles and the main nave, by means of arched apertures, is a reason for the non-exponential energy decay that is characteristic of large cathedrals or basilicas. Mosques, in contrast, have a square plan layout, and the side aisles, which are

[a)]Electronic mail: zuhre@mezzostudyo.com

 0001-4966/2016/140(1)/344/12/$30.00

limited in number, are separated from the main prayer zone by large arches. Thus, mosques are more symmetrical than basilicas and are composed of a single unfragmented volume. Another difference between Christian worship spaces and mosques is that the former have a stone cladded reflective floor and mosques have a carpeted, more absorptive floor.

In this study, a historical worship space in İstanbul, namely, the Süleymaniye Mosque, with its great size and multi-domed design, is chosen as a case for non-exponential sound decay investigations. Experimental data were collected through field tests. The collected data are then investigated for non-exponential decay characteristics using Bayesian analysis. For a better understanding of the mechanisms of non-exponential decay, diffusion equation modeling is applied for sound energy flow vector analysis.

Acoustic coupling has been studied and observed before in coupled spaces and cathedrals/basilicas. The major difference between a typical coupled volume space and the Süleymaniye Mosque is that the receiver in the present study is not in the room with lower reverberation, in which the energy subsequently reaches from the highly reverberant main space. On the contrary, the receivers are in the middle of the main space, or prayer zone, where all energy interactions take place. The main difference between acoustical coupling investigations in cathedrals and in the Süleymaniye Mosque is that the fragmented spaces and totally reflective basilican layouts of Christian worship spaces provide ideal circumstances for non-exponential energy decay to be observed, involving the coupling of side chambers to the main space. The Süleymaniye Mosque, on the other hand, has a dominant *single space* and a carpeted floor surface.

The literature shows that in single-volume spaces with a non-homogenous material distribution, non-diffuse sound fields may arise. The non-exponential energy decay observed within such enclosures may be due to this non-diffuse sound field.[14,30] Mosques are symmetrical single space enclosures having a highly reflective upper-structure coupled to an absorptive floor, and they might induce non-exponential sound energy decay. This hypothesis should be validated; after that, the factors and mechanisms involved can be identified. Most previous work in room acoustics coupling generates data from scale model tests or computer simulations. The field is still improving and more experimental data are needed from real architectural venues, as here.

This paper is structured as follows. Section II sets out the major architectural features of the Süleymaniye Mosque. Section III specifies the data collection methods and the analysis used, including field measurements, the diffusion equation model (DEM) in room acoustics, and Bayesian decay analysis. In Sec. IV, the results are discussed. Section V concludes the paper by emphasizing the major findings.

II. THE SÜLEYMANİYE MOSQUE

The Süleymaniye Mosque and its complex was the largest of the Ottoman building enterprises of its time and was decreed by *Süleyman the Magnificent* and designed by Mimar Sinan, the architect laureate of the Ottoman Empire. The main construction took place during the years 1550–1557. The Süleymaniye Mosque is the centerpiece of the complex (Fig. 1). The mosque is covered centrally by a single dome that is supported on two sides by semidomes. Side aisles are sheltered by five smaller domes, which complete the upper structure.

The Süleymaniye Mosque has an approximate interior volume of 100 000 m^3. The inner plan of the mosque is a rectangle measuring ~63 m × 69 m. The main dome, of diameter 26.20 m, rests on four elephant feet. The height of the dome from the ground to the keystone is 47.75 m. The middle and corner domes on the side aisles have a diameter of 9.90 m, and the others have a diameter of 7.20 m. Apart from the elephant feet, there are eight columns carrying secondary arches. The corner domes are supported by arches between the elephant feet and exterior shell walls.[31,32] Prominent architectural features of the interior are historical columns, marble panels, porphyry discs, great arches, the *mihrab*, *minbar* (pulpit), *müezzin's mahfili*, the royal box (sultan's *mahfili*), stained glass windows, and inscriptions. *Pendentives* are utilized to smooth the central dome, the secondary half dome, and the arch connections. *Muqarnases* made of gypsum are located in the skirting of the half dome and side-dome arch transitions, which enhance sound diffusion in the mainly concave transition planes (Fig. 1).

There is a richness of materials used in the Süleymaniye Mosque. The interior walls are faced with stone revetments, which were delivered from ruins of ancient cities all over the world.[33,34] The columns are made of Egyptian porphyry. The *mihrab* and *minbar* are made of carved white marble and have stained glass windows on the sides. The ceilings of

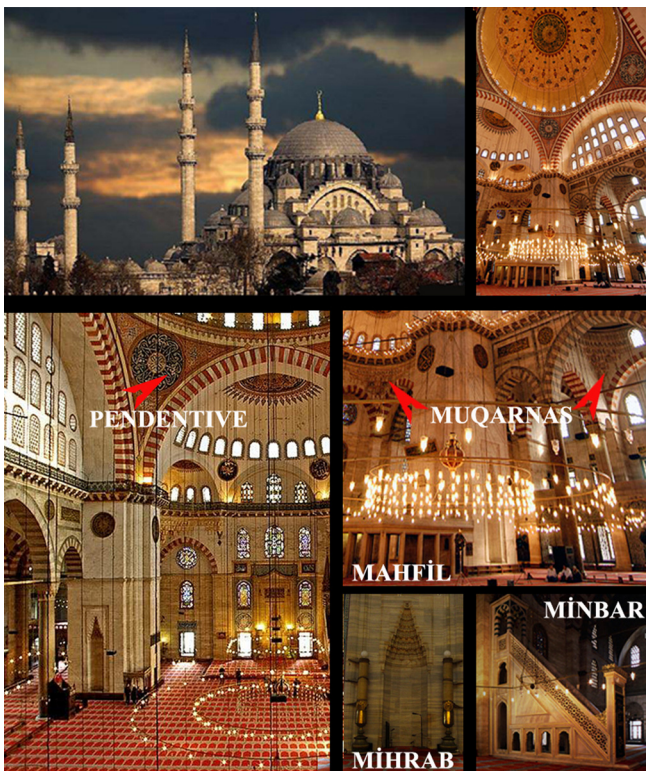

FIG. 1. (Color online) Süleymaniye Mosque and the Complex, İstanbul, 1550–1557, largest of the Ottoman building enterprises of the time, designer: Sinan the Architect; exterior view and interior views.

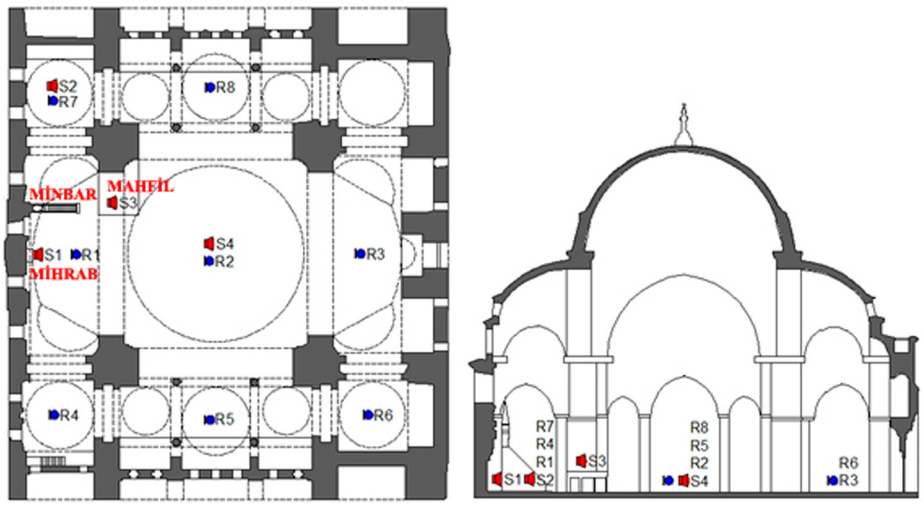

FIG. 2. (Color online) Süleymaniye Mosque field tests source (S) and receiver (R) locations; plan view (left), section view (right).

the *minbar* and the royal box, the domed superstructure, and the *pendentives* are painted. Brick is used as the core material of the domes because of its lightness. The painted brick domes were then decorated with gold foiled pen paintings (Fig. 1). In contrast to the lavishly painted domes and *pendentives* in the lower zones, the stone revetments are relatively bare. Limestone is the main structural stone, as well as the facing stone, for interior walls and wall footings. Lime, *horasan*, fine sand, gypsum, linen, and straw are the basic ingredients of the original plaster layers and seams.[34] Wood is used in the interior mostly for flat ceilings, doors, window frames, and furniture. The floor of the mosque is covered with a carpet.

III. METHODOLOGY

A. Field measurements

Field tests of the Süleymaniye Mosque took place during the night of 23–24 February 2013, within the empty main prayer hall during the night when there was minimum background noise (environmental, traffic, etc). To estimate the basic parameters specifying the sound field, the room impulse responses were collected. The equipment used was in accordance with ISO 3382–1.[35] A Brüel & Kjær (B&K, Nærum, Denmark) (type 4292-L) standard dodecahedron omni-directional sound source was used for acoustic excitation with a B&K (type 2734-A) power amplifier. The room impulse responses at various measurement points were captured by a B&K (Type 4190ZC-0032) microphone. The sampling frequency of the recorded multi-spectrum impulse was 48 kHz. The height of the omni-directional sound source was 1.5 m off the floor, and the microphone height was always 1.2 m. The B&K DIRAC Room Acoustics Software type 7841 v.4.1 was used to generate differing noise signals.

When measuring a room impulse response, the measurement quality is limited in part by background noise, which can significantly influence all parameter values that can be estimated from the impulse responses. The level of any reliable decay range is significant in multi-slope decay analysis. In the Süleymaniye Mosque tests, the aim was to obtain a signal that is at least 50 dB higher than the noise floor in the octave bands of interest (peak-to-noise ratio, PNR $>$ 50 dB). For the same reason, while acquiring signals with least distortion and highest PNR, an exponential-sweep source signal was used for all the measurements. The duration of collection of the room impulse responses was 21.8 s, which is long enough to avoid time aliasing.

The major source locations were in front of the *mihrab* (S1) and at the *müezzin's mahfili* (S3), both of which are traditional *imam* or *müezzin* positions in a mosque (Figs. 2 and 3). For the room acoustics coupling investigation, further source locations were used, including underneath the main dome (S4) and side corner domes (S2). Eight receiver locations (R1–R8) were combined with four source locations (S1–S4), giving rise to the measured source-receiver configurations as shown in Figs. 2 and 3. For the differing microphone-source configurations, with multiple times of recording for different pre-average tests, a total of 83 impulse responses were obtained.

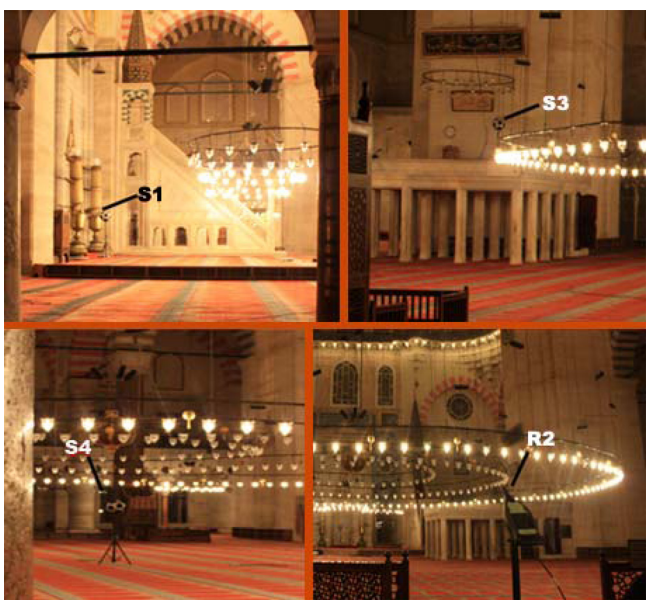

FIG. 3. (Color online) Süleymaniye Mosque field measurement photographs, 23 February 2013.

B. Diffusion equation model (DEM)

In this research, the DEM is applied in a real superstructure to study room acoustics coupling. This model is computationally efficient, and a useful tool in flow vector and spatial energy density analysis inside the entire volume. The DEM applies for enclosures with diffusely reflecting boundaries, in which the rate of change involved in diffusion is slow.[36] The Süleymaniye Mosque has diffusely reflective walls and upper shell structure, all these surfaces are assigned a sound absorption coefficient of 0.09 for octave frequency band of 1 kHz. A low sound absorption coefficient ($\alpha_{1\ \mathrm{kHz}}$ 0.23) of the floor comprises a small fraction of the interior surfaces. This assignment of low absorption coefficient to the carpeted floor through a modified boundary condition [as discussed below in Eq. (6)] is based on adjustment of overall reverberation times from the DEM compared with the field measurement results. The modified boundary condition suits situations where a small portion of surfaces is moderately absorptive or one boundary absorbs a portion of the sound energy.[37] With this modified boundary condition, the DEM is applicable[38] provided that the sound absorption coefficient for the small surface involved is <0.3; this criterion is satisfied by the carpet in the Süleymaniye Mosque for 1 kHz and below. This section of the paper now outlines the interior and boundary equations involved; details of the diffusion equation modeling are given elsewhere.[39–43]

1. Interior diffusion equation

In the presence of an omni-directional sound source within a room region or domain (V) with time-dependent energy density $q(r,t)$, sound energy density (w) at a position (r) and time (t) is defined as[19]

$$\frac{\partial w(r,t)}{\partial t} - D\nabla^2 w(r,t) + cmw(r,t) = q(r,t), \in V, \qquad (1)$$

where ∇^2 is Laplace operator, D is the diffusion coefficient, c is speed of sound, and m is the coefficient of air absorption. The diffusion coefficient D in Eq. (2) takes into account the room morphology via its mean free path (λ)[36,39,40] given by

$$D = \frac{\lambda c}{3} = \frac{4Vc}{3S}, \qquad (2)$$

where λ is the mean free path, V is the volume of the room, and S is the total surface area of the room.

In fact, D may not be always assigned to a "constant" in certain situations, such as in long or elongated rooms, and may be a "variable" depending on room dimensions and the source-receiver positions.[41] The Süleymaniye Mosque has an almost square plan layout and a cubical three-dimensional geometry. Due to its proportionate dimensions, the mean-free-path is considered as being independent on spatial location and D is therefore taken as a constant.

In Eq. (1) the source term $q(r,t)$ is zero for any subdomain in which no source is present. In a time-dependent solution, a point source with an arbitrary acoustic power of $P(t)$ can be modeled as an impulsive sound source as follows:

$$q(r_s,t) = E_0\delta(r-r_s)\delta(t-t_0), \qquad (3)$$

where δ is the Dirac-delta function, r_s denotes the position of the source. E_0 is the energy produced by the source at source location r_s and at time t_0. For practical purposes, a source emitting a constant power P in a short time interval Δt can be considered. Thus, E_0 can be approximated by $E_0 \simeq P\Delta t$.[36]

2. Boundary conditions

The boundary condition that takes into account the energy exchanges on enclosing surfaces is[37]

$$J(r,t)\cdot\boldsymbol{n} = -D\nabla w(r,t)\cdot\boldsymbol{n} = A_X\, cw(r,t), \quad \text{on } S, \qquad (4)$$

where $J(r,t)$ is sound energy flux vector, c is the speed of sound, and A_X is an exchange coefficient, a quantity that involves differing absorption assignments at different surface locations. In coupled spaces, distributed absorption is more accurate than a mean absorption term in the diffusion equation.[20] The Süleymaniye Mosque is a single space structure with a carpeted floor and a reflective upper shell. Thus, its boundary condition corresponds best to the modified mixed boundary model [Eq. (5)].[37] This exchange coefficient can be applied for modeling the local effects of the sound fields having relatively higher absorption on specific surfaces

$$A_X = \frac{\alpha}{2(2-\alpha)}. \qquad (5)$$

The resulting system of boundary equation is

$$-D\frac{\partial w(r,t)}{\partial n} = \frac{c\alpha}{2(2-\alpha)}w(r,t), \quad \text{on } S. \qquad (6)$$

A three-dimensional model of the Süleymaniye Mosque is generated from the most recent architectural survey drawings obtained from the Turkish Republic Prime Ministry Directorate General of Foundations Archive,[32] which reflects the present condition and is suitable for use in the DEM (Fig. 4). The model is fine-tuned with field test results taking

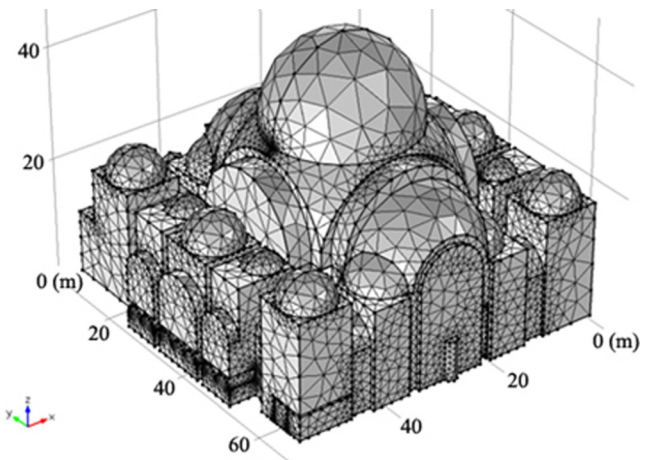

FIG. 4. (Color online) Süleymaniye Mosque solid mesh model; total of 124 788 linear Lagrange-type mesh elements; mesh size; min: 1.12 m, max: 6.20 m; interior volume: ~129 000 m^3.

TABLE I. Süleymaniye Mosque multi-slope analysis results of sample field measurement data; number of decay/slope (S), decay rates (s) over frequency for different source-receiver configurations, where T_1 is the first decay rate, T_2 is the second decay rate, and T_3 is the third decay rate.

		Frequency (Hz)					
Source receiver number		250	500	1000	2000	4000	8000
S_1R_4	Slope number	2	2	2	2	2	3
	Decay rates	T_1:11.5	T_1:5.8	T_1:4.6	T_1:3.9	T_1:2.5	T_1:1.0
		T_2:15.9	T_2:9.1	T_2:6.6	T_2:6.3	T_2:4.0	T_2:1.8
S_2R_2	Slope number	2	2	2	2	2	2
	Decay rates	T_1:11.5	T_1:6.2	T_1:5.7	T_1:4.1	T_1:2.6	T_1:1.6
		T_2:16.0	T_2:10.0	T_2:7.9	T_2:6.7	T_2:4.1	T_2:2.2
S_3R_7	Slope number	3	2	2	2	2	2
	Decay rates	T_1:8.9	T_1:6.2	T_1:5.4	T_1:3.9	T_1:2.5	T_1:1.3
		T_2:13.5	T_2:9.4	T_2:8.0	T_2:6.1	T_2:4.0	T_2:2.0
		T_3:17.1					

the reverberation time ($T30$) into account. Although information on the random-incident sound absorption coefficient for generic materials such as stone, glass, or wood can be found in the literature, the original lime-based plaster finishes in the Süleymaniye Mosque may not match today's cement-based plasters in their acoustic properties, whereas the sound absorption coefficients of marble and the carpet used (of which samples are available) are approximately estimated. In the tuning process, the absorption coefficients assigned to the plasters are adjusted until decay times in simulations match those obtained in field tests.

Next, using a finite element solver, Eqs. (1), (3), and (6) are solved for a total of 124 788 linear Lagrange-type mesh elements, which fulfill the meshing conditions solely governed through the mean-free path of the room,[36] being 18.26 m, and accordingly the mean free time (MFT) of the room is 53 ms [Eq. (2)]. In time-dependent solutions, the resulting values of $w(r,t)$ are used for the spatial sound energy density distribution and sound energy flow vector analysis. According to Fick's law, the gradient of the sound energy density $w(r,t)$ at position r and time t in the room under investigation is proportional to the sound-energy flow vector J. In this study, the local sound energy-density flux $J(r,t)$ is taken as the gradient of the sound energy density apart from a negative sign as[36]

$$J(r,t) = -D\nabla w(r,t). \tag{7}$$

TABLE II. Decay parameters (decay levels and decay times) for impulse responses collected at S_1R_4 filtered for 500 Hz and collected at S_3R_7 filtered for 250 Hz in field tests, where T_1 is the first decay rate, T_2 is the second decay rate, T_3 is the third decay rate, A_0 is the noise term, A_1 is the first decay level, A_2 is the second decay level, and A_3 is the third decay level.

Decay parameters	S_1R_4 500 Hz, field	S_3R_7 250 Hz, field
A_0 (dB)	−85	−86
A_1 (dB)	−6	−8
T_1 (s)	5.8	8.9
A_2 (dB)	−15	−9
T_2 (s)	9.1	13.5
A_3 (dB)	—	−15
T_3 (s)	—	17.1
BIC (db)	53 683 (2 slopes)	68 744 (3 slopes)
BIC (db)	42 126 (1 slope)	42 126 (2 slopes)
BIC_{21}, BIC_{32}, (db)	11 557	26 617

C. Bayesian decay analysis

Sound energy decay analysis of measured room impulse responses is performed in this study via Bayesian probabilistic inference. Bayesian probability theory is a quantitative theory of inference that includes valid rules of statistics for relating and manipulating probabilities. It permits the incorporation of all the available information concerning the parameters of interest.[44] A Bayesian model-based decay analysis,[27] relying on the model approximation of real data based on Schroeder integration,[45] is used in the estimation of multi-rate decay functions. This allows estimation of the number of decay rates without requiring an initial guess of the number of slopes inherent in the decay data, generated by a high level probabilistic inference, model-selection method. Bayesian parameter estimation[27,28] is used to analyze the decay parameters of the decay profile for the selected model.

The Bayesian model analysis is based on the Schroeder decay model, which is a generalized linear model consisting of linear combinations of a number of nonlinear or exponential terms. Schroeder decay functions are obtained through Schroeder backward integration. A generalized linear parametric model (H_S) with S exponential decay terms describing the Schroeder decay function is[27]

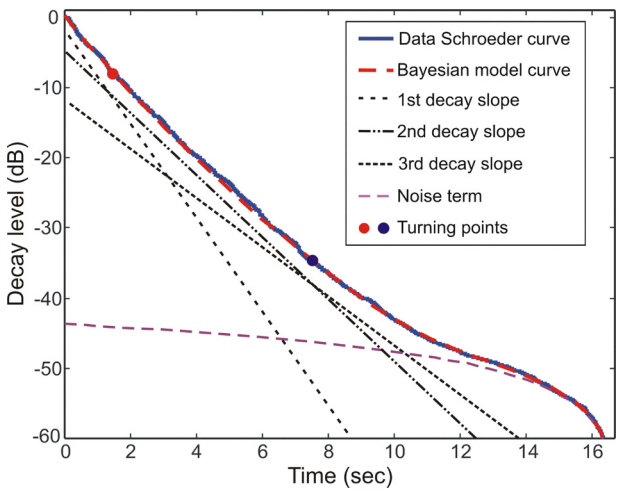

FIG. 5. (Color online) Schroeder curve and the model curve derived from impulse responses collected at S_3R_7 filtered for 250 Hz in field tests. Three decomposed decay slope lines and two turning points are shown.

TABLE III. Comparison of decay parameters (decay levels and decay times) for impulse responses collected at S_1R_4 filtered for 1000 Hz out of field tests, DEM simulations for current state with carpeted floor, and DEM simulations for marbled floor, where T_1 is the first decay rate, T_2 is the third decay rate, A_0 is the noise term, A_1 is the first decay level, and A_2 is the second decay level.

Decay parameters	Field	DEM carpet floor	DEM marble floor
A_0 (dB)	−84	−90	−83
A_1 (dB)	−7	−8	−6
T_1 (s)	4.6	4.9	8.0
A_2 (dB)	−9	−9	—
T_2 (s)	6.6	6.2	—
BIC (db)	62 112 (2 slopes)	1598 (2 slopes)	—
BIC (db)	27 195 (1 slope)	1376 (1 slope)	2141 (1 slope)
BIC_{21} (db)	34 917	221	–

$$H_S(A, T, t_i) = A_0(t_K - t_i) + \sum_{j=1}^{S} A_j\left(e^{-13.8 t_i/T_j} - e^{-13.8 t_K/T_j}\right), \quad (8)$$

where index $0 \le i \le K-1$. The decay parameters A_j: $A_1, A_2, A_3, \ldots$ are the linear amplitude parameters and are related to the level of individual exponential decay terms when expressed logarithmically. T_j are the decay times associated with the logarithmic decay slopes of individual exponential decay terms with $j = 1,2,\ldots,S$, where S is the number of exponential decay terms, also termed *decay orders*. $A_0(t_K - t_i)$ is a noise term and t_K is the upper limit of the Schroeder integration, where the subscript K is the total number of data points,[27] and t_i with a lowercase subscript i represents the discrete time variable.

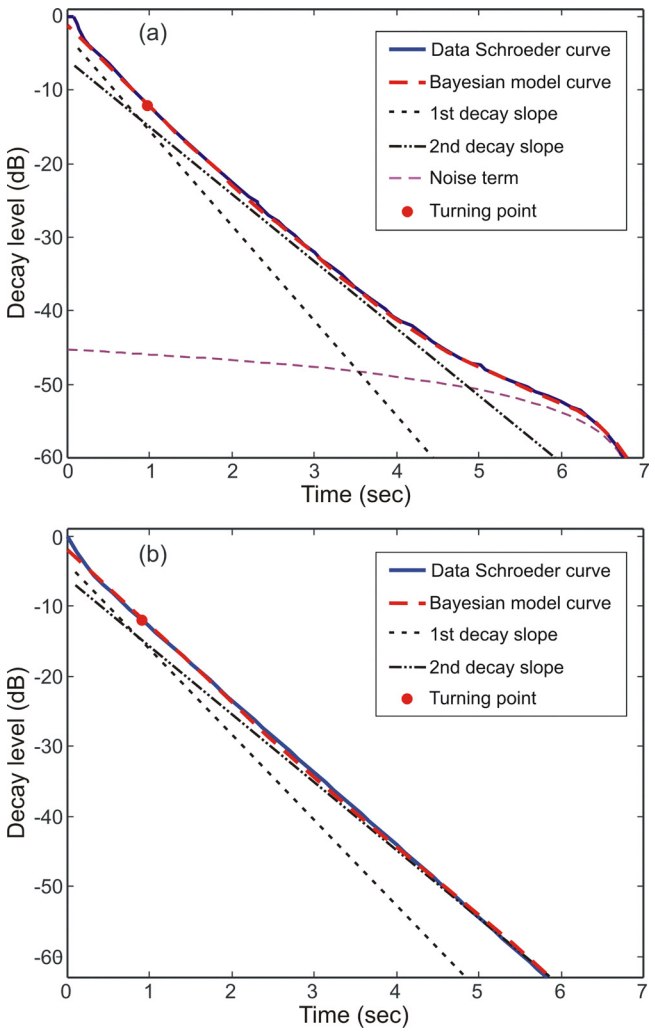

FIG. 6. (Color online) Field (a) versus DEM (b) results for S_1R_4; double-slope model derived from the room impulse responses, band pass-filtered at 1 kHz. Two decomposed decay slope lines and one turning point are shown.

To determine how many decay slopes are contained in the energy decay data has always been a challenge. Straightforward curve fitting inevitably leads to over-parameterized models, because increased decay orders always improve curve fitting. Xiang *et al.*[27] proposed instead to evaluate the Bayesian evidence on the model-selection level, a procedure which automatically encapsulates the principle of parsimony and quantitatively implements Ockham's razor principle. The Bayesian implementation of Ockham's razor prefers simpler models and penalizes over-fitting. In the energy decay analysis, among a set of decay models, the model yielding the largest Bayesian information criterion (BIC) or approximated evidence is considered to be the most concise model providing the best fit to the decay function data while capturing the important exponentially decaying features contained in the data.[27]

IV. RESULTS AND DISCUSSION

A. Bayesian decay analysis of experimental data

In this section, decay parameter estimations are performed and discussed for room impulse responses obtained in the field tests. Typical results for the field measurements are given in Table I, including decay times and the number of exponential decay terms estimated by the Bayesian analysis for different source-receiver configurations. The BIC values are compared for double- and triple-slope cases. A higher BIC value is associated with a specific number of slopes indicating the most likely number of decay terms (Table II). Ockham's razor prefers the simpler model, so that, for comparatively close BIC values, or in quantitative terms when one BIC after conversion to decibans (db)[46] is not at least 10 db greater than the other, then the decay rate with the simpler model is selected.

Double slopes are predominant in overall measurement locations, and triple slopes are rarely observed. Table II presents a complete list of decay parameter values of one double-slope and one triple-slope decay cases. These include room impulse responses collected in field tests at S_1R_4 (where S_x stands for source and R_x stands for receiver number), filtered for 500 Hz, and at S_3R_7, filtered for 250 Hz. The Schroeder decay curve derived from the room impulse response at S_3R_7 filtered for 250 Hz is shown in Fig. 5 with decomposed decay slopes and turning points indicated on the graph.

Data collected at S_1R_4 indicate double slopes for all analyzed octave bands between 250 Hz and 8 kHz (Table I), which is the typical pattern in the overall field test results. In data collected at S_1R_4 and filtered for 250 Hz, the decay levels are well separated and decay times differ clearly from

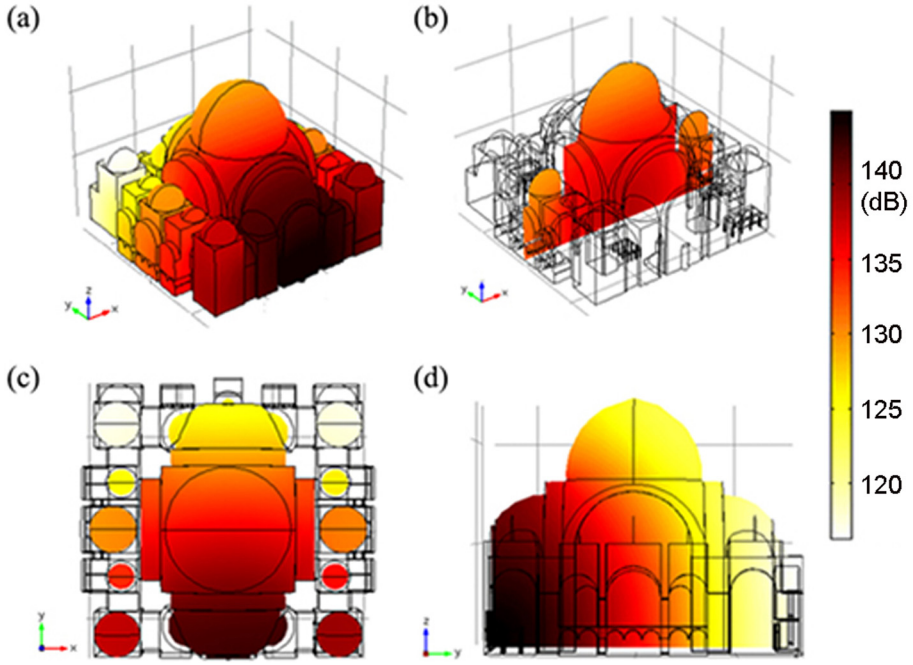

FIG. 7. (Color online) Spatial sound energy level (dB) distribution, time: 0.1 s, 1 kHz; volume and slice plots of Süleymaniye Mosque DEM solution (a) axonometric view; (b) section parallel to the *mihrab* wall, central axis; (c) plan view; (d) section through the *mihrab* wall, central axis.

each other (Table II). The BIC value of the double-slope model for S_1R_4 is much higher than for the single-slope case. For field data collected at S_3R_7 and filtered for 250 Hz, the decay times are well separated and the BIC of the triple-slope model is 26 617 db higher than that of a double-slope model (Table II). Thus, this data can be confidently taken as indicating a triple-slope (Fig. 5).

Studies of decay parameters in the Süleymaniye Mosque based on experimental data indicate multi-slope decay characteristics within this superstructure. This result confirms that even single-space venues having specific geometric attributes and material distributions can create non-diffuse sound fields leading to a convex-curved curvature in sound energy decay.[14,30]

B. Simulated versus field-measured data

The DEM is used to confirm the non-exponential energy decay patterns observed in the field tests. The DEM is also used to investigate the influence of interior material configurations in generating non-diffuse sound fields. To experiment with the effects of material type, the Süleymaniye Mosque's carpeted floor was replaced with a marbled floor in DEM simulation.

Sound energy impulse responses are calculated for some critical receiver locations in the DEM solution and compared to the field test results for the same locations. As an example, T_1 (the first decay time) and T_2 (the second decay time) obtained at S_1R_4 filtered for 1 kHz in field tests is compared

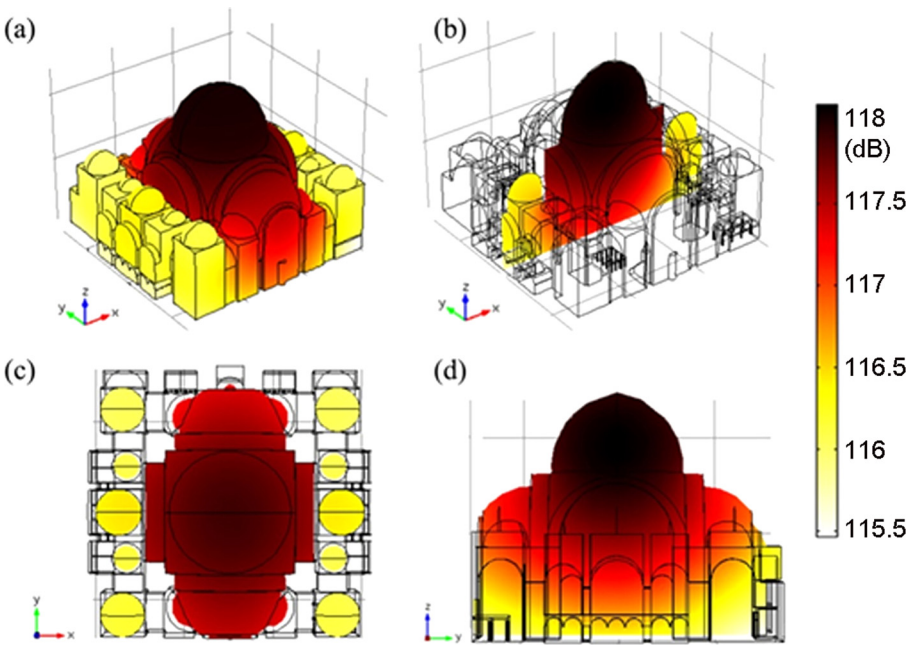

FIG. 8. (Color online) Spatial sound energy level (dB) distribution, time: 2 s, 1 kHz; volume and slice plots of Süleymaniye Mosque DEM solution (a) axonometric view; (b) section parallel to the *mihrab* wall, central axis; (c) plan view; (d) section through the *mihrab* wall, central axis.

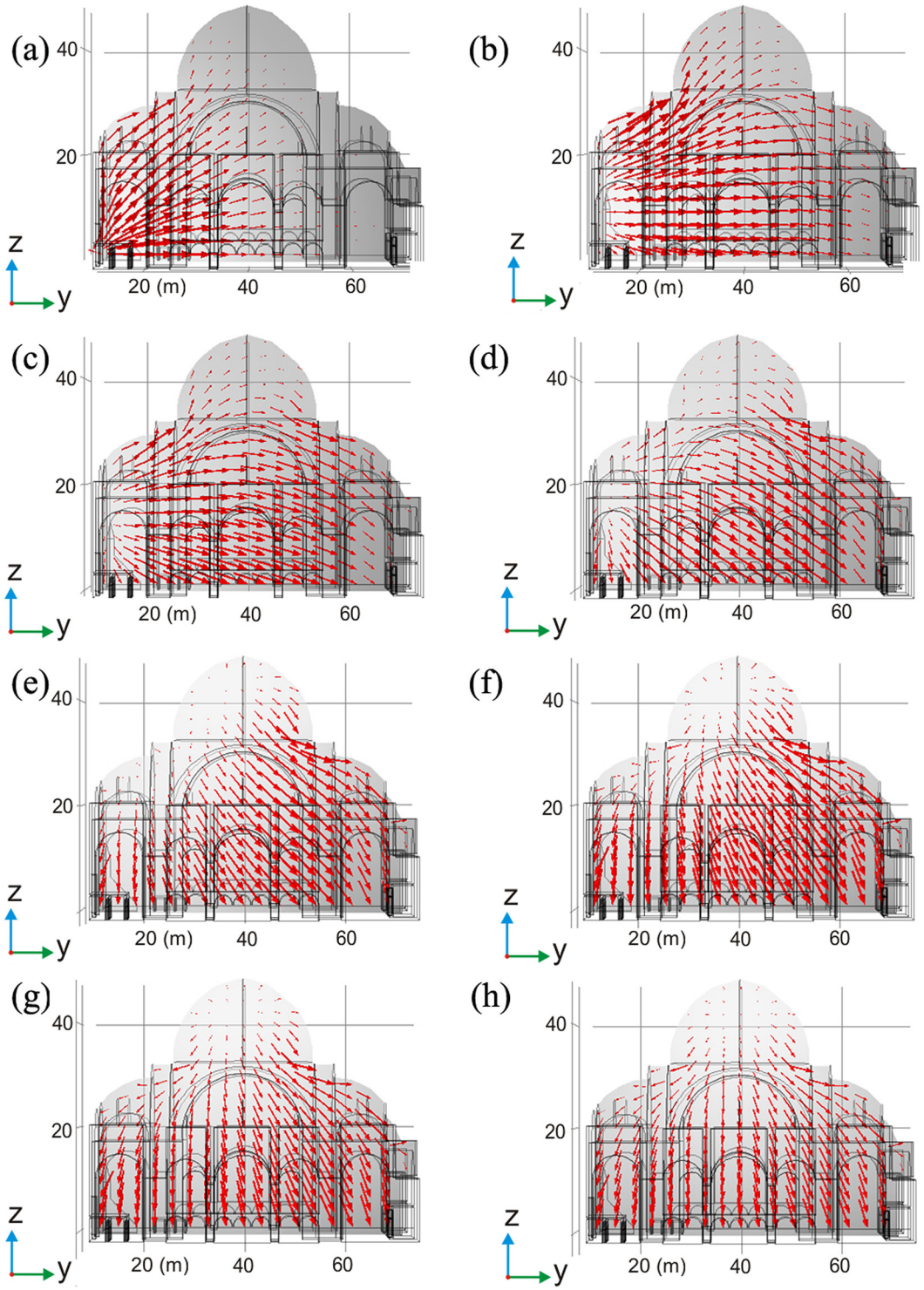

FIG. 9. (Color online) Two-dimensional mapping of sound-energy flow vectors (arrow surface plots) for 250 Hz. (a) Time: 0.1 s, (b) time: 0.2 s, (c) time: 0.3 s, (d) time: 0.4 s, (e) time: 0.5 s, (f) time: 0.6 s, (g) time: 0.7 s, (h) time: 0.8 s, Süleymaniye Mosque present condition.

to T_1 and T_2 of the impulse response obtained via the DEM solution for S_1R_4 filtered for 1 kHz. The results for T_1 and T_2 both agree well with the observed and DEM-solved impulse responses (see Table III and Fig. 6). In fact, the decay rate (or the slope) for the first decay time (T_1) need not coincide with $T30$. This depends on where the early decay is crossed/overlapped with later decay(s).

An important finding for this specific position (S_1R_4) is that neither the field nor the DEM data are single-slope cases; rather they comprise double-slope characteristics. In Fig. 6, the curve difference in the later decay shapes is a result of the noise term (background noise) that is present in the field tests, whereas in the DEM simulated data there is no noise to interfere with the impulse response. Figure 6 indicates that the field and DEM results both support the double-slope form within the superstructure for that particular receiver-source configuration, for the present state of the mosque with carpet floor finish.

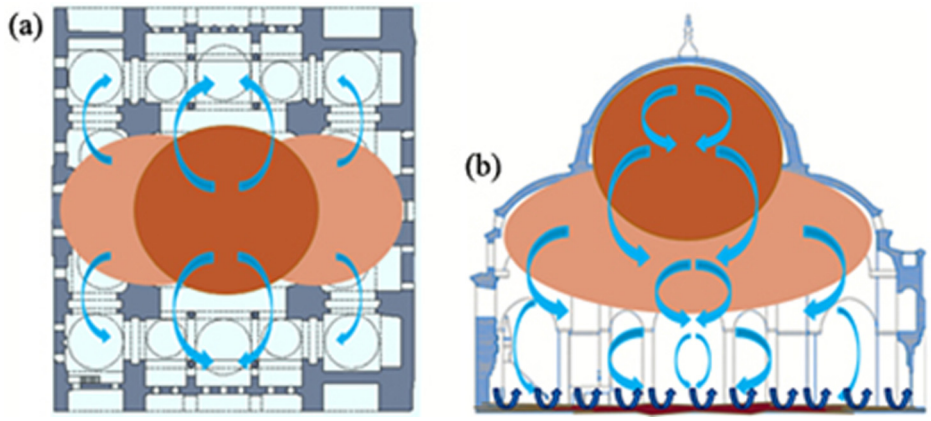

FIG. 10. (Color online) Conceptual plan (a) and section (b) views of energy zones in the Süleymaniye Mosque. The energy concentration zone is the volume at the upper half of the mosque sheltered by the central dome over pendentives, which is in between four elephant feet. The energy deficient zones are the side aisles and the prayer area over the floor surface.

Table III also lists the DEM solution results at position S_1R_4 filtered for 1 kHz when the floor material is changed from carpet to marble. For this specific source-receiver configuration, the Süleymaniye Mosque with carpet floor gives rise to double-slope decays, whereas a marble floor for position S_1R_4 filtered for 1 kHz results in a single-slope sound energy decay. Section IV C discusses this finding in detail.

C. Spatial sound energy distribution and flow pattern

To shed light on the physics of multi-slope decay in this structure, the interior sound field is visualized via the spatial sound energy distribution and energy flow analysis. This section discusses the results obtained.

For a sound source located centrally in front of the *mihrab* wall, Fig. 7 illustrates the sound energy density distributions for 1 kHz and for the time 0.1 s—right after the termination of the sound source. Around this time, the sound energy density is concentrated at the front part of the *mihrab* wall, where the point source is simulated. The energy begins to flow from the *mihrab* wall toward the back of the prayer hall. The sound energy density is higher closer to the floor (receiver/prayer heights) beneath the central dome than at prayer locations in front of the back wall, and is least underneath the back wall corner domes and upper back half of the central dome (Fig. 7). Figure 8 shows the sound energy density distributions at time 2 s (±100 ms) for 1 kHz. The high energy concentration at the upper central dome, and comparatively energy deficient zones by side aisles and floor surfaces, are clearly observed in the spatial sound energy distribution plots in Fig. 8.

The main reason of providing spatial sound energy distribution plots is to better visualize the sound energy flows. Rather than the sound energy level differences (or absolute difference between the maximum and the minimum in dB), the pattern of energy flows within the volume is sought. Regardless of the magnitude of this absolute difference in sound energy levels, the energy would still drain from the energy dense volume/zone to the scarce zone. The accumulation of energy in the upper section of the mosque contributes to the overlapping of early and late energy decays, particularly in areas closer to the floor.

Following the spatial energy distributions, energy flows are investigated by a flow vector analysis based on the DEM solution from which the energy flow vectors are derived by Fick's law [Eq. (7)]. The energy flow vectors derived from

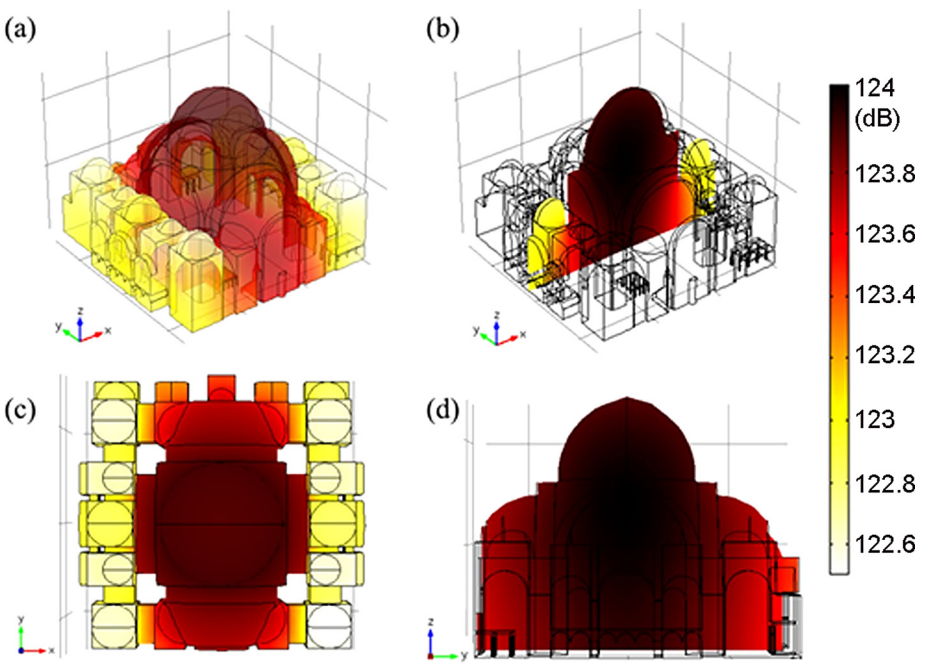

FIG. 11. (Color online) Spatial sound energy level (dB) distribution, marble floor scenario for 1 kHz, time: 2 s. (a) Axonometric view; (b) section parallel to the *mihrab* wall, central axis; (c) plan view; (d) section through the *mihrab* wall, central axis.

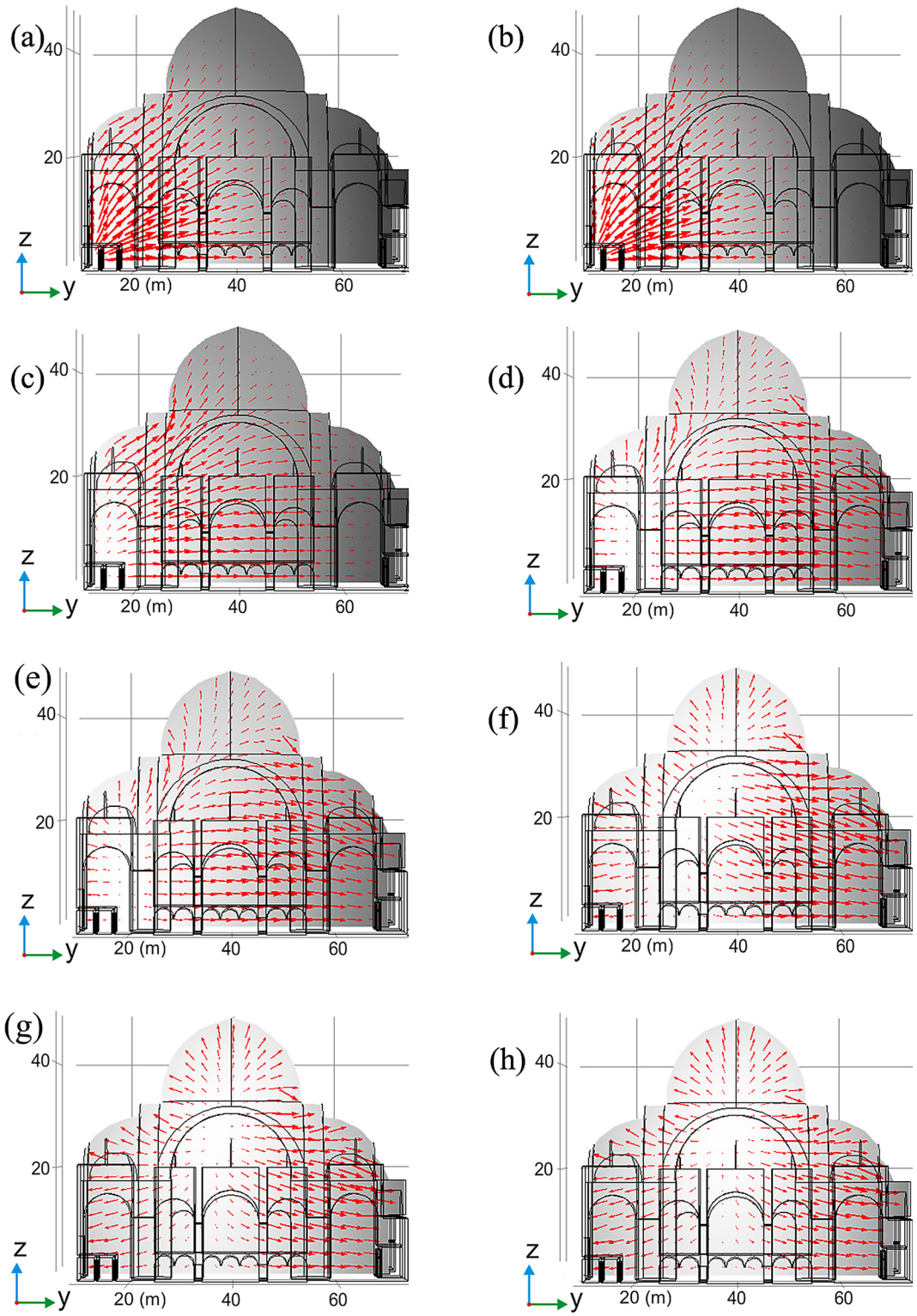

FIG. 12. (Color online) Süleymaniye Mosque two-dimensional mapping of sound-energy flow vectors, marble floor scenario for 1 kHz. (a) time: 0.1 s, (b) time: 0.2 s, (c) time: 0.3 s, (d) time: 0.4 s, (e) time: 0.5 s, (f) time: 0.6 s, (g) time: 0.7 s, (h) time: 0.8 s.

the DEM solution facilitate investigations of the energy fluxes and their flow direction reversal. Previous work[19] using DEM simulations verified that the energy flow-direction changes occur at the turning points of multi-sloped sound-energy decays estimated via Bayesian analysis. The directional characteristics of flow vectors in a time-dependent solution can serve as an indicator of multi-slope sound energy decay.

For the time-dependent solution at 250 Hz, Fig. 9 shows vector surface plots of the Süleymaniye Mosque DEM solution, for the section crossing the center of the *mihrab* wall. The time interval between 0.1 s and 0.8 s is shown, with a time step of 0.1 s. After 1 s, the flow vector directions do not deviate very much. With a focal point at the center of the main dome, the sound energy keeps flowing toward the rest

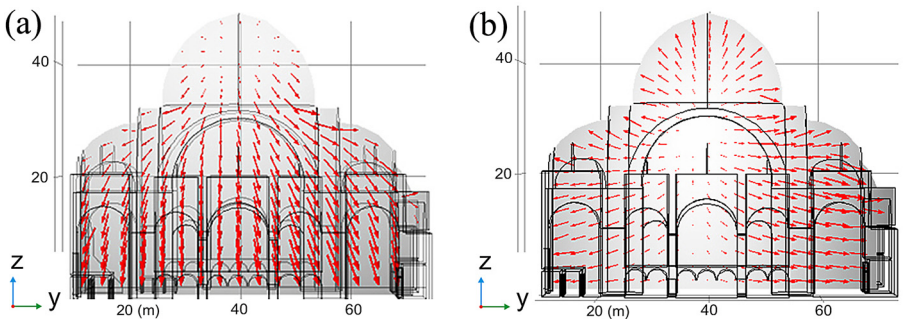

FIG. 13. (Color online) Sound-energy flow vector distribution comparison of Süleymaniye Mosque floor finishes for section through the *mihrab* wall, central axis, time: 2 s; carpet floor (a) versus marble floor (b).

of the mosque's prayer zones. Absorption by the floor attenuates the sound in regions closer to the floor, so that the energy density in that area is lower than in the upper portion. In contrast, with its reflective surfaces and focusing geometry the energy accumulation center, the main dome, feeds back sound energy to the floor area, serving as a reverberant "coupled volume" within this single-space structure. The architectural features of the mosque, specifically the reflective central dome combined with a relatively absorptive prismatic base, create two geometric zones for sound diffusion/propagation (Fig. 10). This is the main reason for the multi-slope decay pattern observed in this structure.

The acoustic effect of floor absorption is better analyzed in comparison with a reflective floor. The carpet floor finish of the Süleymaniye Mosque is replaced with marble in DEM and the model is re-solved with this change of material. For lower octave bands, the difference between the sound absorption performance of the carpet and the marble is small. The difference is more obvious in higher octave bands. For that reason, Figs. 11 and 12 illustrate 1 kHz solution for spatial sound energy distributions and flow vectors.

Figure 11 illustrates the DEM solution of the spatial sound energy distributions at time 2 s for the marble floor. The central zone under the main dome does not participate in a significant breakup of the energy distribution on the *mihrab* wall axis. Figure 12 shows the flow vectors corresponding to the DEM solution for times between 0.1 s and 0.8 s, with a time step of 0.1 s. At the end of this time interval the energy is concentrated at the center of the whole structure, with arrows directed from the central axis of the structure to the boundaries of the mosque.

Figure 13 shows that the basic difference between the carpeted floor and bare marble floor is the location of the energy center. For the carpeted floor, the focal point is the center of the main/central dome, whereas for the bare marble floor the focus is not a point but an axis passing from the center of the floor in plan to the midpoint of the main dome. In the marbled floor scenario, the energy flows from the central axis toward the side walls of the mosque. This creates a highly symmetric and even distribution, or flow of sound energy within the structure, and prevents multi-slope decay.

This outcome follows not only from the spatial energy distribution and energy flow vector analysis, but also from estimates of the decay parameters, as set out in Table III. The results highlight the significance of the relatively absorptive floor material in comparison to a reflective upper wall and ceiling structure. This results in the uneven and non-diffuse distribution of the sound field and, consequently, multi-slope energy decay in a single space monumental structure. These discussions all relate to the unoccupied space, to facilitate correlation of DEM solutions with the experimentally measured data. For the case when the floor of the mosque is fully occupied, as in Friday's sermon, the separation zones of the energy fragmentation will be greater because sound absorption near the floor will be increased. The multi-slope decay will therefore occur more often when the mosque is occupied.

V. CONCLUSIONS

A key concern of this study is to confirm that a multiple-slope energy decay profile can occur in an oversize *single space* structure having a particular geometry and distribution of materials. In particular, a multi-domed structure, the Süleymaniye Mosque, has been analyzed. The methodology involves *in situ* acoustical measurements. The mechanism of multi-slope decays is investigated by applying the diffusion equation model (DEM) in a finite-element scheme. Spatial sound energy distributions and energy flows are analyzed by means of the DEM. Bayesian analysis is used to estimate the multiple-slope decay parameters. The investigations of energy decay in the Süleymaniye Mosque based on measured impulse response data have confirmed that even a single space structure with particular geometrical features and material configurations can induce multi-slope sound energy decays.

Major outcomes of this study are as follows:

- Uneven distribution of sound absorption within the space, even for a slight difference of absorption, has provided the circumstances for non-exponential energy decay observation. Immense volume and large surface areas emphasize the effect of minor differences of material characteristics.
- The large size of the domical superstructure and its reflective interior surface, in comparison to relatively absorptive prayer floor, support the late energy flow leading to non-exponential energy decay.
- The consequence of non-diffuse sound field is the multi-slope decay pattern observed inside the Süleymaniye Mosque, which is supported by both field tests and DEM simulations.

In this study, supplemented by Bayesian analysis, the diffusion equation modeling has revealed the mechanism for the multi-slope decay pattern. The DEM

application in this case study has proved to be a powerful method, particularly for in-depth sound energy flow analysis. Such numerical methods, applied in parallel with field measurements, can motivate and accelerate future room acoustics analyses with possible non-exponential decay profiles.

ACKNOWLEDGMENTS

The authors would like to express their sincere appreciation to Professor Ayşe Tavukçuoğlu for her guidance in this study and to Professor Yun Jing for his valuable advice. Our gratitude is extended to the General Directorate of Pious Foundations of Turkey (T.C. Vakıflar Genel Müdürlüğü) for providing the measured drawings of the Süleymaniye Mosque and for giving permission to collect field measurements. MEZZO Stüdyo Ltd. in Ankara should also be acknowledged for providing acoustical measurement equipment used in field tests.

[1]A. A. El-khateeb and M. R. İsmail, "Sounds from the past: The acoustics of Sultan Hassan Mosque and Madrasa," Build. Acoust. **14**(2), 109–132 (2007).
[2]Z. Sü and S. Yilmazer, "The acoustical characteristics of the Kocatepe Mosque in Ankara, Turkey," Arch. Sci. Rev. **51**(1), 21–30 (2008).
[3]A. A. Abdou, "Measurement of acoustical characteristics of mosques in Saudi Arabia," J. Acoust. Soc. Am. **113**(3), 1505–1517 (2003).
[4]P. Fausti, R. Pompoli, and N. Prodi, "Comparing the acoustics of mosques and Byzantine churches," *CIPA XIXth International Symposium*, Antalya, Turkey (2003).
[5]A. P. Carvalho and C. G. Monteiro, "Comparison of the acoustics of mosques and Catholic churches," in *ICSV16*, Kraków, Poland (2009).
[6]K. Abdelazeez, R. N. Hammad, and A. A. Mustafa, "Acoustics of King Abdullah Mosque," J. Acoust. Soc. Am. **90**(3), 1441–1445 (1991).
[7]H. A. Hamadah and H. M. Hamouda, "Assessment of speech intelligibility in large auditoria case study: Kuwait State Mosque," Appl. Acoust. **54**(4), 273–289 (1998).
[8]R. Su'arez, J. J. Sendra, J. Navarro, and A. L. León, "The acoustics of the Cathedral-Mosque of Córdoba, proposals for architectural intervention," Acta Acust. **90**, 362–375 (2004).
[9]Z. Sü Gül and M. Çalışkan, "Impact of design decisions on acoustical comfort parameters: Case study of Doğramacızade Ali Paşa Mosque," Appl. Acoust. **74**, 834–844 (2013).
[10]N. Prodi and M. Marsilo, "On the effect of domed ceiling in worship spaces: A scale model study of a mosque," Build. Acoust. **10**(2), 117–134 (2003).
[11]M. Kleiner, D. L. Klepper, and R. R. Torres, *Worship Space Acoustics* (Ross, Fort Lauderdale, FL, 2010).
[12]J. C. Jaffe, "Multipurpose performance halls," in *The Acoustics of Performance Halls: Spaces for Music from Carnegie Hall to the Hollywood Bowl* (Norton, New York, 2010), Chap. 9, pp. 98–111.
[13]C. F. Eyring, "Reverberation time measurements in coupled rooms," J. Acoust. Soc. Am. **3**(2), 181–206 (1931).
[14]L. Cremer and H. A. Müller, "Coupled rooms," in *Principles and Applications of Room Acoustics* (Elsevier, London, 1978), Vol. 1, pp. 261–292.
[15]E. N. Wester and B. R. Mace, "A statistical analysis of acoustical energy flow in two coupled rectangular rooms," Acta Acust. **84**, 114–121 (1998).
[16]J. S. Anderson and M. B. Anderson, "Acoustic coupling effects in St. Paul's Cathedral, London," J. Sound and Vib. **236**(2), 209–225 (2000).
[17]F. Martellotta, "Identifying acoustical coupling by measurements and prediction-models for St. Peter's Basilica in Rome," J. Acoust. Soc. Am. **126**(3), 1175–1186 (2009).
[18]A. Billon, V. Valeau, A. Sakout, and J. Picaut, "On the use of a diffusion model for acoustically coupled rooms," J. Acoust. Soc. Am. **120**(4), 2043–2054 (2006).
[19]N. Xiang, Y. Jing, and A. C. Bockman, "Investigation of acoustically coupled enclosures using a diffusion-equation model," J. Acoust. Soc. Am. **126**(3), 1187–1198 (2009).
[20]P. Luizard, J. D. Polack, and B. F. G. Katz, "Sound energy decay in coupled spaces using a parametric analytical solution of a diffusion equation," J. Acoust. Soc. Am. **135**(5), 2765–2776 (2014).
[21]C. M. Harris and H. Feshbach, "On the acoustics of coupled rooms," J. Acoust. Soc. Am. **22**(5), 572–578 (1950).
[22]M. Meissner, "Computational studies of steady-state sound field and reverberant sound decay in a system of two coupled rooms," Cent. Eur. J. Phys. **5**(3), 293–312 (2007).
[23]L. Nijs, G. Jansens, G. Vermeir, and M. Voorden, "Absorbing surfaces in ray-tracing programs for coupled spaces," Appl. Acoust. **63**, 611–626 (2002).
[24]J. E. Summers, R. R. Torres, and Y. Shimizu, "Statistical-acoustics models of energy decay in systems of coupled rooms and their relation to geometrical acoustics," J. Acoust. Soc. Am. **116**(2), 958–969 (2004).
[25]J. E. Summers, R. R. Torres, Y. Shimizu, and B. L. Dalenback, "Adapting a randomized beam-axis tracing algorithm to modeling of coupled rooms via late-part ray tracing," J. Acoust. Soc. Am. **118**(3), 1491–1502 (2005).
[26]N. Xiang, P. Robinson, and J. Botts, "Comment on 'Optimum absorption and aperture parameters for realistic coupled volume spaces determined from computational analysis and subjective testing results' [J. Acoust. Soc. Am. **127**, 223–232 (2010)]," J. Acoust. Soc. Am. **128**, 2539–2542 (2010).
[27]N. Xiang, P. M. Goggans, T. Jasa, and P. Robinson, "Bayesian characterization of multiple-slope sound energy decays in coupled-volume systems," J. Acoust. Soc. Am. **129**(2), 741–752 (2011).
[28]N. Xiang and P. M. Goggans, "Evaluation of decay times in coupled spaces: Bayesian parameter estimation," J. Acoust. Soc. Am. **110**(3), 1415–1424 (2001).
[29]A. C. Raes and G. G. Sacerdote, "Measurements of the acoustical properties of two Roman basilicas," J. Acoust. Soc. Am. **25**(5), 954–961 (1953).
[30]H. Kuttruff, "Coupled rooms," in *Room Acoustics* (Spon, London, 2000), pp. 142–145.
[31]D. A. Kuban, "Symbol of Ottoman architecture: The Süleymaniye," in *Ottoman Architecture* (Antique Collectors' Club, Suffolk, UK, 2010), pp. 277–294.
[32]*Süleymaniye Mosque Documents* (T. R. Prime Ministry Directorate General of Foundations Archive, Ankara, Turkey, 2011).
[33]G. Necipoğlu-Kafadar, "The Süleymaniye Complex in İstanbul: An interpretation," Muqarnas **3**, 92–117 (1985).
[34]I. A. Kolay and S. Çelik, "Ottoman stone acquisition in the mid-sixteenth century: The Süleymaniye Complex in İstanbul," Muqarnas **23**, 251–272 (2006).
[35]ISO 3382-1 (R2009), "Acoustics—Measurement of reverberation time of rooms with reference to other acoustical parameters" (International Organization for Standardization, Geneva, Switzerland, 2009).
[36]V. Valeau, J. Picaut, and M. Hodgson, "On the use of a diffusion equation for room-acoustic prediction," J. Acoust. Soc. Am. **119**(3), 1504–1513 (2006).
[37]Y. Jing and N. Xiang, "On boundary conditions for the diffusion equation in room acoustic prediction: Theory, simulations, and experiments," J. Acoust. Soc. Am. **123**(1), 145–153 (2008).
[38]N. Xiang, J. Escolano, J. M. Navarro, and Y. Jing, "Investigation on the effect of aperture sizes and receiver positions in coupled rooms," J. Acoust. Soc. Am. **133**(6), 3975–3985 (2013).
[39]J. Picaut, L. Simon, and J. D. Polack, "A mathematical model of diffuse sound field based on a diffusion equation," Acta Acust. **83**, 614–621 (1997).
[40]A. Billon, J. Picaut, and A. Sakout, "Prediction of the reverberation time in high absorbent room using a modified-diffusion model," J. Appl. Acoust. **69**, 68–74 (2008).
[41]C. Visentin, N. Prodi, V. Valeau, and J. Picaut, "A numerical investigation of the Fick's law of diffusion in room acoustics," J. Acoust. Soc. Am. **132**(5), 3180–3189 (2012).
[42]Y. Jing and N. Xiang, "A modified diffusion equation for room-acoustic predication," J. Acoust. Soc. Am. **121**(6), 3284–3287 (2007).
[43]J. Escolano, J. M. Navarro, and J. J. López, "On the limitation of a diffusion equation model for acoustic predictions of rooms with homogeneous dimensions," J. Acoust. Soc. Am. **128**(4), 1586–1589 (2010).
[44]N. Xiang and C. Fackler, "Objective Bayesian analysis in acoustics," Acoust. Today **11**(2), 54–61 (2015).
[45]M. R. Schroeder, "New method of measuring reverberation time," J. Acoust. Soc. Am. **37**, 409–412 (1965).
[46]J. Escolano, N. Xiang, J. M. Perze-Lorenzo, M. Cobos, and J. J. Lopez, "A Bayesian direction-of-arrival model for an undetermined number of sources using a two-microphone array," J. Acoust. Soc. Am. **135**(2), 742–753 (2014).